Dynamics of direct X-ray detection processes in high-Z Bi_2O_3 nanoparticles-loaded PFO polymer-based diodes

A. Ciavatti, T. Cramer, M. Carroli, L. Basiricò, R. Fuhrer, D. M. De Leeuw, and B. Fraboni

Citation: Appl. Phys. Lett. **111**, 183301 (2017);
View online: https://doi.org/10.1063/1.4986345
View Table of Contents: http://aip.scitation.org/toc/apl/111/18
Published by the American Institute of Physics

Dynamics of direct X-ray detection processes in high-Z Bi_2O_3 nanoparticles-loaded PFO polymer-based diodes

A. Ciavatti,[1] T. Cramer,[1] M. Carroli,[1] L. Basiricò,[1] R. Fuhrer,[2] D. M. De Leeuw,[3] and B. Fraboni[1]

[1]*Department of Physics and Astronomy, University of Bologna, Viale Berti Pichat 6/2, Bologna 40127, Italy*
[2]*Avantama AG, Laubisrutistrasse 50, 8712 Stafa, Switzerland*
[3]*Faculty of Aerospace Engineering, Delft University of Technology, Kluyverweg 1, 2629 HS Delft, The Netherlands*

(Received 4 June 2017; accepted 17 October 2017; published online 30 October 2017)

Semiconducting polymer based X-ray detectors doped with high-Z nanoparticles hold the promise to combine mechanical flexibility and large-area processing with a high X-ray stopping power and sensitivity. Currently, a lack of understanding of how nanoparticle doping impacts the detector dynamics impedes the optimization of such detectors. Here, we study direct X-ray radiation detectors based on the semiconducting polymer poly(9,9-dioctyfluorene) blended with Bismuth(III)oxide (Bi_2O_3) nanoparticles (NPs). Pure polymer diodes show a high mobility of 1.3×10^{-5} cm^2/V s, a low leakage current of 200 nA/cm^2 at -80 V, and a high rectifying factor up to 3×10^5 that allow us to compare the X-ray response of a polymer detector in charge-injection conditions (forward bias) and in charge-collection conditions (reverse bias), together with the impact of NP-loading in the two operation regimes. When operated in reverse bias, the detectors reach the state of the art sensitivity of 24 μC/Gy cm^2, providing a fast photoresponse. In forward operation, a slower detection dynamics but improved sensitivity (up to 450 ± 150 nC/Gy) due to conductive gain is observed. High-Z NP doping increases the X-ray absorption, but higher NP loadings lead to a strong reduction of charge-carrier injection and transport due to a strong impact on the semiconductor morphology. Finally, the time response of optimized detectors showed a cut-off frequency up to 200 Hz. Taking advantage of such a fast dynamic response, we demonstrate an X-ray based velocity tracking system. *Published by AIP Publishing.*
https://doi.org/10.1063/1.4986345

Organic semiconductors combine efficient charge transport with low-temperature deposition on plastic substrates, large-area processing, and elastic material properties. This unique combination of features makes them a promising class of materials to build large-area and flexible ionizing radiation detectors for X-ray imaging or dosimetry.[1,2] The possibility of developing low cost, fast, and large area ionizing radiation detectors is extremely appealing for industrial applications and security purpose (e.g., smart walls in public places or to scan trucks at national borders). However, up to now, the maximum detector size is 17 in., limited by the technology of materials' growth at high quality over a large area; moreover, they are heavy, rigid, and expensive and require high temperature (>700 °C) in the fabrication process. In this view, organic materials would represent a resource for their easy, low temperature, and low-cost deposition techniques over large surfaces. Indeed, organic semiconductors have been employed as solution-processed direct X-ray detectors in the form of single crystals,[3–5] microcrystalline thin films,[6] or conjugated polymer thin films.[7–9] In analogy to traditional solid state detectors, organic semiconductor detectors rely on the collection of charge carriers generated in the semiconductor as a consequence of high energy photon absorption and subsequent ionization processes. While the charge collection processes in organic semiconductors can be efficient due to fast transport and low exciton recombination, high-energy photon absorption is challenging as organic materials are constituted of atoms with low atomic numbers (low-Z). Polymer composites have been introduced by Mills *et al.* with the aim of combining the efficient charge transport of a semiconducting polymer matrix with strong high-energy photon absorption by nano- or microparticles made of heavy atoms (high-Z),[10] enhancing the sensitivity of a factor 4 [e.g., from 141 nC/Gy cm^3 for a nanoparticle (NP)-free 5 μm polymer-based device to 468 nC/Gy cm^3 for a 57 wt. % Bi_2O_3 NP load device]. More recently, a similar approach has also been reported by Ankah *et al.*, which presented an hybrid–organic direct X-ray photodetector fabricated using inorganic lead sulfide (PbS) nanocrystal quantum dots blended in a polymer matrix.[11] A different concept has been instead presented by Büchele *et al.*,[8] demonstrating that scintillating terbium-doped gadolinium oxysulfide (GOS:Tb) X-ray absorbers blended in a polymer bulk heterojunction create a quasi-direct X-ray detector with a sensitivity up to 459 e^-/nGy mm^2 (corresponding to 7.34 μC/Gy cm^2). An additional possibility to increase the X-ray sensitivity is offered by photoconductive gain that has been recently introduced to organic semiconductor detectors.[6] Exploiting such an approach, our group very recently reported about a highly sensitive (up to 1200 nC/Gy) X-ray detector based on a low-voltage organic field-effect transistor.[12] In contrast to pure charge collection, photoconductive gain requires injecting contacts in order to produce a steady state current that gets modulated by X-ray generated charge density.

The combination of both strategies, high-Z absorbers and photoconductive gain, is at the core of signal amplification and improves sensitivity in a semiconducting polymer

detector. We demonstrate the fabrication of high-performing polymer diodes with a very efficient rectification ratio using a MoO_3 based charge injection layer doped with high-Z nanoparticles (NPs) to improve X-ray absorption. These devices allowed us to compare the X-ray response of a polymer detector in charge-injection conditions (forward bias) and in charge-collection conditions (reverse bias), together with the impact of NP-loading in the two operation regimes. Our findings emphasize the crucial role of electrode-semiconductor interface barriers in the tuning of organic X-ray detector performance and allow us to interpret the detection mechanism and to make clear the specific role of NP-loading in the two different operation modes.

Polymer diodes were prepared by spin-coating of a dispersion of poly(9,9-dioctyfluorene) (PFO) and Bi_2O_3 NPs (Avantama) in toluene (2 wt. % of polymer) on Cr/Au bottom electrodes. As hole injection and top contact layers, MoO_3 and Al were thermally evaporated. We chose PFO as an active layer of the devices because it is operationally and environmentally stable, it has high hole mobility, and it is also a well-known polymer used as a hole transport layer in organic light emitting diodes.[13] Moreover, it is much cheaper than polymers already employed as direct X-ray detectors [such as PTAA, poly(triaryl amine)]. The Bi_2O_3 nanoparticles have been chosen for their high atomic number. We tested also other combinations of polymers and NPs, but the PFO/Bi_2O_3 blend resulted to be the best performing one. Figure 1 shows the band energy diagram of the device and a scheme of the diode structure and the current-voltage characteristics of diodes for the increasing NP content. The pure-polymer diode achieves a strong rectification factor of

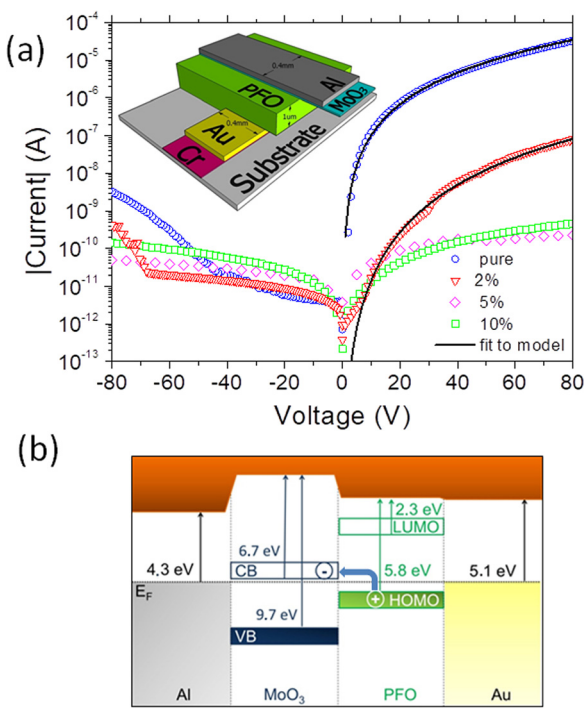

FIG. 1. Structure and electrical properties of semiconducting polymer diodes: (a) IV curves of 1.5 μm-thick diodes (different layer thicknesses are reported in Fig. SI1 in the supplementary material) with different contents of Bi_2O_3 NPs and fit of curves to the space charge limited current model. The sketch of the diode's architecture is shown in the inset. (b) Energy band diagram.

3×10^5 with an off-current of 200 nA/cm^2 at -80 V. The current in forward bias at low voltages obeys Ohm's law. Above 5 V, the space-charge limited current (SCLC) regime sets in and the current increases superlinearly. The measured exponential behavior is well explained by space charge effects in a disordered polymer diode as described analytically by Torricelli.[14] Figure 1(b) (black continuous line) shows the power-law fit matching experimental data. The average hole mobility for pure PFO results to be $(1.3 \pm 0.5) \times 10^{-5}$ cm^2/V s, in excellent agreement with the literature.[15] The strong rectification factor confirms the efficient hole charge injection at the MoO_3 layer, whereas a Schottky junction at the PFO/Au interface acts as a barrier for the transport in reverse bias operation.

NP doping of 2, 5, and 10 wt. % leads to a strong deterioration of diode forward current, as shown in Fig. 1(b). At 50 V, the rectification factor reduces from 10^5 of pristine PFO to about 1 for 10 wt. % blended devices. The Torricelli diode transport model is still applicable to 2 wt. % and results in a mobility of $(3.3 \pm 1.2) \times 10^{-7}$ cm^2/V s, that is, two orders of magnitude lower than in the pure polymer. NP concentrations above 10 wt. % lead to inhomogeneous polymer films due to NP agglomeration. The structural analysis of the polymer/NP films (XRD, TEM, and AFM, see supplementary material) confirms the presence of dispersed, Bi_2O_3 nanoparticles with an average diameter value of 18 nm and the presence of pure polymer crystalline domains in the composite thin film. As the amount of NPs increases, these polymer domains disappear, and AFM images (supplementary material) show that they are substituted by small NP agglomerates with a diameter in the range of 70–100 nm, which lead to the degradation of charge transport properties of the semiconducting polymer. In addition, we suggest that the formation of interfacial NP agglomerates deteriorates charge injection into the polymer, thus decreasing the rectification properties of the doped polymer diode.

X-ray photocurrent measurements were performed with an X-ray tube (Mo target, 35 kV). Figure 2(a) shows the photocurrent response of pure PFO diodes biased at ± 80 V which were exposed for 10 s to increasing X-ray dose rates. The stability of the measured response has been assessed over more than five repetitions (see Fig. SI3 in the supplementary material). In forward operation (blue dots), a continuous increase in photocurrent during the exposure time is observed. After closing the shutter, the current decays to the background level on a similar timescale. We attribute such a strong but slow response to a photoconductive gain process (see below). In contrast, in reverse operation (red line), the diode produces an immediate, but one order of magnitude smaller, photocurrent response that remains constant throughout exposure. This response in the reverse operation regime is due to the collection of generated excess charges separated in the depletion region by the electric field, without contribution of charge injection, as will be better discussed and supported in the following.

The effect of high-Z nanoparticle doping on the forward and reverse operation regimes of the detector is shown in Figs. 2(b)–2(d). In reverse operation, the shape of the photocurrent transient maintains its box shape; however, two significant effects can be noticed: (i) the dark current drops with

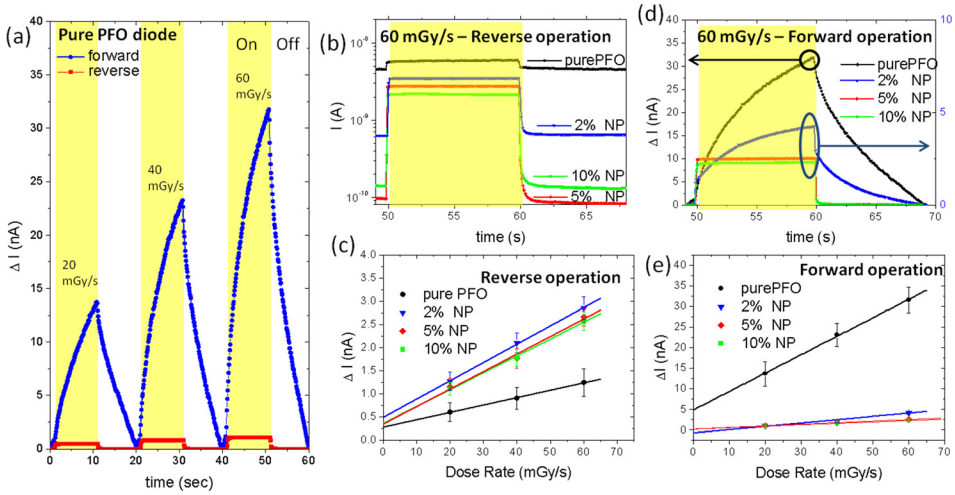

FIG. 2. X-ray detection with pure and NP-blended polymer diodes. (a) Characteristic X-ray photocurrents in a 1 μm thick pure PFO diode. The dark currents have been subtracted for comparison. (b) Impact of NPs on diode detector properties in reverse bias. (c) Photocurrent against the dose-rate for diodes operated in reverse bias. NP blended diodes show the largest X-ray sensitivity. (d) Impact of NPs on diode photocurrent response in forward bias. (e) Photocurrent against the dose-rate for diodes operated in forward bias. Photocurrents of the pure PFO diode increase by more than one order of magnitude with respect to reverse operation.

the increasing NP concentration and (ii) a larger photocurrent variation $I_{ON} - I_{OFF}$ (ΔI) is present in the NP doped polymer diodes. All detectors show a linear response at increasing dose rates D with the highest sensitivity $S = d\Delta I/dD$ and largest photocurrents obtained for 2 wt. % NP doping [Fig. 2(c)]. In forward operation, the effect of NPs on detector performance is more pronounced: the photocurrent transient shows a transition from the saw-tooth like shape of the pure diode to a rectangular shape with increasing NP-concentrations. This is associated with one order of magnitude reduction in photocurrent, sensitivity, response time, and dark current. The response in forward operation as a function of the dose rate is also linear [Fig. 2(e)]. Table I summarizes the detector properties of the polymer diodes for both operation regimes. From these data, we identify the pure-PFO diode in forward operation as the detector with the largest sensitivity $S = 450 \pm 140$ nC/Gy. The 2 wt. % NP-doped diode in reverse operation shows the highest performance ratio of photocurrent and dark-current, combined with reasonable sensitivity.

The investigation of the speed of response is essential to assess the possible applications for these detectors and to better understand the physical processes involved in the detection mechanism. The X-ray flux on the polymer diode was modulated using a mechanical shutter, and the photocurrent signal was amplified using a FEMTO current amplifier. Under reverse bias conditions, the photoresponse remains constant up to frequencies of 40–60 Hz and then starts to decay following a power-law with a critical exponent of 0.5 [Fig. 3(a)]. In forward bias, the photocurrent response is much slower, and still at frequencies down to 0.04 Hz, no saturation of the signal is observed and follows the same power-law as the reverse bias diode. Doping with high-Z NPs has a significant impact on the detector dynamics when operated under reverse bias [Fig. 3(b)]: fast and constant photoresponses in the low frequency range and an increased amplitude due to improved X-ray absorption are observed. The amount of NPs also changes the power-law that describes the decay at higher frequencies. The detector rise times, evaluated by photocurrent transient measurements, are in the range of 5–8 ms and confirm these findings, in agreement with cut-off frequencies (at -3 dB) in the 120–200 Hz range (see Table I and Fig. SI4 in the supplementary material).

The combination of Al/MoO_3 and Au based contact electrodes enables highly rectifying diodes, which allow us to address the investigation of X-ray photocurrent generation under injecting and non-injecting conditions in the same single device. Without carrier injection (reverse bias), the photocurrent results from the separation and collection of ionization charges generated by X-ray photon absorption and other secondary processes in the semiconductor. Therefore, the photocurrent intensity is directly proportional to the X-ray flux and remains constant during X-ray exposure. The response rise time is fast (<10 ms) as it depends only on the timescale necessary to transport charges to the collecting electrodes. When carrier injection occurs (forward bias), instead, a constant space charge limited background current is present in the device due to injection from the MoO_3/Al electrode. Upon X-ray exposure, the photocurrent rises continuously with exposure time due to photoconductive gain, allowing us to achieve one order of magnitude increase in detector sensitivity. Such a gain effect has been explained and modelled in organic semiconductors by employing the trapping of negative charge carriers. Here, we suggest a similar mechanism, which bases on the fact that PFO is a hole-transporter but traps electrons.[16] Therefore, excitons

TABLE I. X-ray sensitivities of polymer diodes at forward and reverse bias operation for the 1 μm-thick PFO layer.

			REVERSE (−80V)			FORWARD (+80V)		
NP-content (wt. %)	Mobility (cm^2/V s)	Rise time (ms)	S (nC/Gy)	I_{dark} (A)	$\Delta I/I_{dark}$	S (nC/Gy)	I_{dark} (A)	$\Delta I/I_{dark}$
0	$(1.3 \pm 0.5) \times 10^{-5}$	7.84	16 ± 1	3.6×10^{-9}	0.34	450 ± 140	3.6×10^{-5}	8.8×10^{-4}
2	$(3.3 \pm 1.2) \times 10^{-7}$	5.11	39 ± 1	4×10^{-10}	7.13	80 ± 15	7.9×10^{-8}	5.4×10^{-2}
5	n.a.	7.24	38 ± 4	5×10^{-11}	53.2	37 ± 3	2.2×10^{-10}	11.4
10	n.a.	7.43	36 ± 2	6×10^{-11}	33.4	34 ± 1	4.5×10^{-10}	5.1

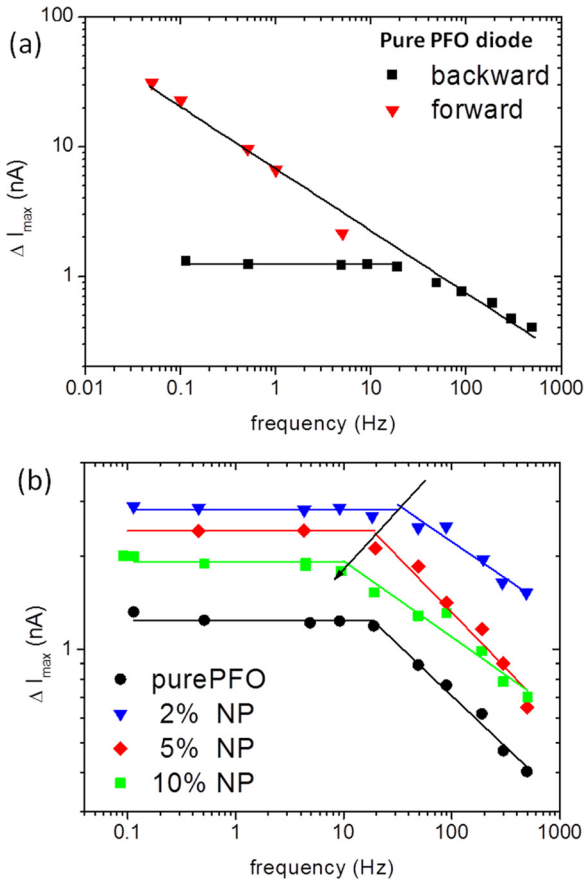

FIG. 3. Analysis of polymer diode detector dynamics. The plot of the amplitude of the photocurrent response as a function of the shutter frequency for pure and doped diodes is shown. (a) Comparison between the pure PFO diode operated under forward and reverse bias conditions. (b) Impact of the NP concentration on detection with reverse bias. The photoresponse starts to decrease at 10–100 Hz, and a higher NP concentration leads to slightly slower detector dynamics: the black arrow highlights the shift to lower cut-off frequencies at higher NP concentrations.

generated by X-rays dissociate due to the electric field, but, when electrons get trapped in the organic semiconductor, additional holes need to be continuously emitted from the injecting electrode (MoO_3 layer) to maintain charge neutrality. Therefore, a photoconductive gain process is activated and a much larger X-ray induced photocurrent is obtained, as described in more detail in Ref. 6. In the forward bias mode, the photocurrent signal is slow and follows a saw-tooth shape whose timescale is dominated by the life-time of the electron traps.

It is noteworthy that we can assess both regimes in a single device. Previously reported polymer-based X-ray detectors, which considered only one regime of operation, ascribe the observed slow dynamic response[8,17] to trap states at the electrode/polymer interfaces. Following our results, we can now assume that the slow response is due to a combination of charge carrier injection/trapping and photoconductive gain effects. In this view, we can further interpret the experimental outcome reported by Intaniwet *et al.*[17] as follows: the response time is fast when the blocking barrier is high, and it decelerates (and the signal higher in amplitude) as the electrode becomes more injecting. The photoconductive gain effect is indeed dominant in the detection process of organic devices, not only based on the bis-(triisopropylsilylethynyl)pentacene film[6] but also on single-crystals, where fast and slow X-ray responses have been observed for low and high mobility molecules, respectively.[18] Importantly, the initial mechanisms that lead to exciton generation and charge separation in the semiconductor due to X-ray absorption are identical in both operation regimes. Although both regimes differ by one order of magnitude on the characteristic time scale and sensitivity, the same power-law describes the decay of photocurrents when beyond cut-off frequency [see Fig. 3(a)].

The addition of NPs has two significant effects on the diode operation. First, the charge carrier mobility in the bulk of the semiconductor reduces probably due to a reduction in nanocrystalline polymer domains. Second, charge injection gets blocked, and thus, a strong reduction in the rectification ratio and a decrease in reverse current are observed. We assume that the occurrence of NP aggregates at the electrode interfaces at higher NP loading is responsible for this effect. From the detector point of view, the addition of small amounts of NPs is beneficial when operated under reverse bias because the higher content of high Z atoms leads to a stronger X-ray photon absorption and increased sensitivities. At the same time, the reduction in reverse dark-current improves the signal to noise ratio. Higher loadings of NPs still improve absorption; however, charge transport and extraction become limiting and start to overweight the improvements in absorption already at a loading of 5 wt. %. The forward regime, instead, is very sensitive to good transport properties, and the NP doping strongly suppresses the photoconductive gain effect already at a concentration of 5 wt. %, when the detector response relies purely on the extraction of primarily generated-charge carriers.

The NP doped diodes show fast response to X-ray exposure, reaching a rise time of 5 ms for the 2 wt. % NP loading. Such values are much faster than the responses of the hybrid organic-inorganic photodiode employing scintillating NPs,[8] and they are close to the values reported for fast organic single crystals.[4] The fast dynamic response of direct NP-enriched x-ray photodiodes opens the possibility of dynamic X-ray monitoring. To demonstrate the possibility of dynamic X-ray monitoring in a simple application scenario, we employ two adjacent diodes of an array to monitor the velocity of an object moving in front of the array [Fig. 4(a)]. The two diodes were placed at a pitch of 5 mm and operated simultaneously. The rotating object (shutter) moves along the indicated velocity vector and causes repeated exposures of the two diodes at different times. Accordingly, we measure a delay of 5 ms in the fast photoresponse of the second photodiode as shown in Fig. 4(b), which corresponds to a detected velocity of 1.02 ± 0.05 m/s.

To summarize, we fabricated highly rectifying diodes based on the semiconducting polymer PFO that work as direct X-ray detectors in two operation regimes. When operated in reverse bias, they reach the state of the art sensitivity of 24 μC/Gy cm^2, providing a fast, box-shaped photoresponse. In forward operation, a slower kinetics has been observed but provides a sensitivity two orders of magnitude higher than in reverse bias. The simultaneous observation of both regimes in the same device granted clear discrimination and interpretation of the parameters controlling each detection mechanism. The addition of high-Z nanoparticles to the

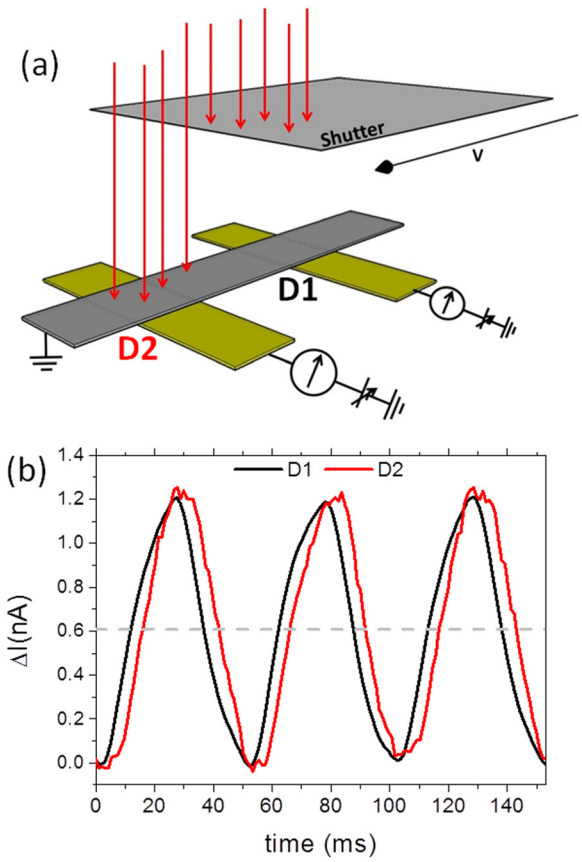

FIG. 4. Velocity measurement with a polymer diode detector array. (a) Schematic of the measurement setup. During aperture and closure, the shutter moves along the direction indicated by the velocity vector, exposing the diodes at different irradiation times. (b) Transient photoresponse obtained from both diodes showing a phase shift.

semiconductor leads to different effects in the two operation regimes: in reverse operation, the photocurrent is increased up to a loading of 5 wt. % NP. In forward operation, no improvement is observed as the conductive gain effect breaks down due to the surface agglomeration of NPs and weakened charge injection. An interpretation of the detection mechanism in both operation regimes has been proposed based on the extraction of photo-generated carriers (reverse bias operation) and on the modulation of photoconductivity by a photoconductive gain process (forward bias operation). Our results highlight the fundamental processes that impact the dynamics of polymer diode X-ray detectors and understanding of which is crucial to achieve high-performance flexible X-ray detectors.

See supplementary material for the additional data and plots reported in the manuscript.

The authors acknowledge the financial support from the European Community under the FP7-ICT Project "i-FLEXIS" (2013-2016).

[1]J. T. Bushberg and J. M. Boone, *The Essential Physics of Medical Imaging* (Lippincott Williams & Wilkins, 2011).
[2]F. Nava, G. Bertuccio, A. Cavallini, and E. Vittone, Meas. Sci. Technol. **19**, 102001 (2008).
[3]B. Fraboni, A. Ciavatti, F. Merlo, L. Pasquini, A. Cavallini, A. Quaranta, A. Bonfiglio, and A. Fraleoni-Morgera, Adv. Mater. **24**, 2289 (2012).
[4]A. Ciavatti, E. Capria, A. Fraleoni-Morgera, G. Tromba, D. Dreossi, P. J. Sellin, P. Cosseddu, A. Bonfiglio, and B. Fraboni, Adv. Mater. **27**, 7213 (2015).
[5]A. Ciavatti, P. J. Sellin, L. Basiricò, A. Fraleoni-Morgera, and B. Fraboni, Appl. Phys. Lett. **108**, 153301 (2016).
[6]L. Basiricò, A. Ciavatti, T. Cramer, P. Cosseddu, A. Bonfiglio, and B. Fraboni, Nat. Commun. **7**, 13063 (2016).
[7]C. R. Newman, H. Sirringhaus, J. C. Blakesley, and R. Speller, Appl. Phys. Lett. **91**, 142105 (2007).
[8]P. Büchele, M. Richter, S. F. Tedde, G. J. Matt, G. N. Ankah, R. Fischer, M. Biele, W. Metzger, S. Lilliu, O. Bikondoa, J. E. Macdonald, C. J. Brabec, T. Kraus, U. Lemmer, and O. Schmidt, Nat. Photonics **9**, 843 (2015).
[9]F. A. Boroumand, M. Zhu, A. B. Dalton, J. L. Keddie, P. J. Sellin, and J. J. Gutierrez, Appl. Phys. Lett. **91**, 033509 (2007).
[10]C. A. Mills, H. Al-Otaibi, A. Intaniwet, M. Shkunov, S. Pani, J. L. Keddie, and P. J. Sellin, J. Phys. D: Appl. Phys. **46**, 275102 (2013).
[11]G. N. Ankah, P. Büchele, K. Poulsen, T. Rauch, S. F. Tedde, C. Gimmler, O. Schmidt, and T. Kraus, Org. Electron. **33**, 201 (2016).
[12]S. Lai, P. Cosseddu, L. Basiricò, A. Ciavatti, B. Fraboni, and A. Bonfiglio, Adv. Electron. Mater. **3**, 1600409 (2017).
[13]C. Zhang, H. von Seggern, K. Pakbaz, B. Kraabel, H.-W. Schmidt, and A. J. Heeger, Synth. Met. **62**, 35 (1994).
[14]F. Torricelli, D. Zappa, and L. Colalongo, Appl. Phys. Lett. **96**, 113304 (2010).
[15]M. Redecker, D. D. C. Bradley, M. Inbasekaran, and E. P. Woo, Appl. Phys. Lett. **73**, 1565 (1998).
[16]H. T. Nicolai, G. A. H. Wetzelaer, M. Kuik, A. J. Kronemeijer, B. de Boer, and P. W. M. Blom, Appl. Phys. Lett. **96**, 172107 (2010).
[17]A. Intaniwet, C. A. Mills, P. J. Sellin, M. Shkunov, and J. L. Keddie, ACS Appl. Mater. Interfaces **2**, 1692 (2010).
[18]L. Basirico, A. Ciavatti, M. Sibilia, A. Fraleoni-Morgera, S. Trabattoni, A. Sassella, and B. Fraboni, IEEE Trans. Nucl. Sci. **62**, 1791 (2015).